November 1982 LRP 215/82

TRANSPORTATION OF FAR-INFRARED BEAMS FOR USE IN PLASMA DIAGNOSTICS

M.R. Siegrist, I. Kjelberg, and R. Behn

TRANSPORTATION OF FAR-INFRARED BEAMS FOR USE IN PLASMA DIAGNOSTICS

M.R. Siegrist, I. Kjelberg, R. Behn

Centre de Recherches en Physique des Plasmas

Association Euratom - Confédération Suisse

Ecole Polytechnique Fédérale de Lausanne

21, Av. des Bains, CH-1007 Lausanne/Switzerland

ABSTRACT

In this paper we discuss certain aspects concerning the transport and focusing of a high-power far-infrared laser beam into a plasma for Thomson scattering measurements.

To attain the required MW power level in a D_2O laser, it is important to use efficiently the volume of the optically-pumped vapor. The best-known method to achieve this is the use of an unstable resonator which produces a beam with an annular intensity profile. This has a negative effect on the quality of the focused beam and on the intensity profile incident on the beam dump. A system utilizing a cassegrain telescope and spatial filtering techniques is found to be a good solution.

I. INTRODUCTION

Development of far-infrared (FIR) lasers for plasma diagnostic purposes is advancing at a rapid pace. While FIR interferometry with cw lasers can already be considered to be a standard technique for density measurements, scattering experiments (e.g. to determine T_i) have suffered so far from lack of adequate laser power. However, lasers have recently been built or are under construction which almost achieve the required power level of ~1 MW and it is expected that a successful T_i-measurement by this method will be reported in the very near future.

While waveguide structures might be used in the laser cavity, free space propagation is usually chosen for beam transportation to the plasma device. For the design of a transport system involving several mirrors, apertures and focusing elements, one has to be able to compute the beam propagation. While this can often be done with sufficient precision by geometrical or Gaussian optics in the visible, the importance of diffraction effects in the FIR, causing a significant spreading of the beam, calls for a more sophisticated method. Gaussian beam propagation is still applicable as long as the radial Gaussian beam profile can be maintained along the whole beam path. For the particular application discussed in this paper this is, however, not the case for two reasons: (i) to achieve the high powers necessary, FIR oscillators of a large volume are required. Unstable resonators will, therefore, generally be used to match the mode volume to the volume of the active medium. In the commonly used confocal, positive branch, unstable resonator[1] output coupling occurs around the edge of the smaller, convex mirror, resulting in a ring-structured intensity pro-

file. (ii) to keep the cost of the reasonably large mirrors required (of the order of 20 cm diameter) within limits, their diameters will not usually be much larger than the beam diameter and they will, therefore, always clip a fraction of the beam, introducing diffraction effects.

Several methods exist to simulate the propagation of a beam including diffraction effects. It is not the aim of this paper to propose a new method, but existing methods will be compared and evaluated with respect to their use for FIR beam transport. Specific problems such as the conversion of a ring-structured beam profile into a smooth focal spot distribution of Gaussian-like shape will be discussed and tables and graphs will be presented to serve as guidelines for the design of a beam transport system.

II. COMPARISON OF BEAM PROPAGATION CODES

Propagation of optical wave fronts can numerically be treated in two different ways: either by solving the differential wave equation (differential method) or by evaluating the Rayleigh-Sommerfeld diffraction formula which mathematically describes the Huygens-Fresnel principle (integral method). Both methods have been discussed and compared in an earlier paper.[2]

The differential method is suitable for short propagation distances and allows us to include distributed effects such as loss or gain or refractive index nonuniformities. It is, therefore, very useful for mode calculations in resonators with an active medium. With its fixed radial step size it cannot easily be applied to converging

and diverging beams and reaches its limits when the propagation through a focal spot has to be investigated. It is possible to investigate diffraction effects with this method since this is implicitely included in the wave equation. However, the discontinuity introduced in the intensity distribution by an aperture with a sharp edge cannot be handled adequately.

With the integral method the radial step size can be varied from wave-plane to wave-plane. This allows us to compute the intensity distribution in the focal spot of a lens or focusing mirror and its propagation beyond this point. Sharp-edged apertures can be treated, but in order to include non-uniform effects of the medium the beam path has to be divided into short sections. For short propagation distances, however, the Fresnel approximation used to solve the double integrals breaks down. This has been discussed in detail by Southwell.[3]

For the free-space beam transport problems discussed in this paper, both short propagation distances and distributed medium effects are irrelevant, but sharp edged apertures have to be considered. Thus the integral method has been used for most of the numerical results reported.

An efficient method for beam propagation calculations is the spectral approach[4] involving Fourier transforms for which very fast algorithms exist. However, it requires rectangular coordinates while all the profiles discussed here are cylindrically symmetric. If a spatial resolution of the order of 1000 radial steps is desired, the storage requirements of this method usually exceed the capacity of a smaller computer.

Since it is difficult to measure beam profiles accurately in the far infrared and thus to compare results with experiments, at least a comparison of the integral and differential methods can be carried out to obtain information on the accuracy. After all, the methods are based on different mathematical principles.

We have compared beam profiles of a flat ring-shaped initial intensity distribution using a resolution of 1200 radial points for a range of propagation distances. In the calculations reported in this paper the wavelength was 385 μm corresponding to one of the principal emission lines of an optically-pumped D_2O laser. To avoid the problems with discontinuities mentioned earlier, the inner and outer edges of the intensity distribution were slightly smoothed in the way described in Ref. 2. With a beam of 20 cm diameter and a 10 cm diameter hole, beam profiles were practically indistinguishable for propagation distances between 10 cm and 2 m, (see Fig. 1). After 5 m the fine structure (ripples) are slightly different. These differences increase, but even at 20 m the coarse structure is recognizably similar. Only the intensities on axis are noticably different. At 50 m the similarities are lost. While the integral method now shows a smooth almost Gaussian-like profile with a few side-lobes, hence a complete filling-in of the initial hole, the differential method produces a spiky irregular profile which is interpreted as being due to numerical instabilities.

For distances less than 10 cm the rapidly oscillating phase term in the double integral creates trouble. This manifests itself in a ghost intensity profile folded into the real profile. There are probably numerical techniques to avoid this problem, but this was not

further investigated.

The conclusion is that for Fresnel numbers between ~2.5 and ~250 both methods show good agreement. Below this range the integral method only should be used and above the differential method.

III. FILL-IN DISTANCES FOR HOLLOW PROFILES

For an ion temperature measurement by Thomson scattering of pulsed FIR radiation the following points are important for the beam transport: (i) the transport efficiency, (ii) the intensity distribution in the focal spot and (iii) the beam divergence and profile beyond the focal spot. Since it is difficult to achieve the required power levels in the first place, the transport efficiency has to be as high as possible. The beam distribution in the focal spot is important for the scattering process. While side lobes can be tolerated to a certain degree, the area over which scattered radiation can be collected with a given solid angle is limited with heterodyne detection.

Even more important is the beam quality beyond the focal spot. It is well known that the efficiency of Thomson scattering is very low[5] of the order of 10^{-12} to 10^{-15}. The suppression of stray light is therefore of paramount importance. Hence the incident beam has to be dumped very efficiently and this is obviously much easier for a beam with small divergence and a rapidly decaying radial intensity distribution.

If a beam with a ring-structured profile is focused, the quality of the intensity distribution in the focal spot is quite good: a large Gaussian-like central lobe with a few much weaker side lobes. However, this beam emerges from the focal spot with a "memory" of its initial shape. At a distance of two focal lengths from the focusing element the beam has again a hollow profile which is fairly similar to the initial one, as shown in Fig. 2. As pointed out earlier this is not desirable and methods have to be found to improve the beam profile before focusing.

Since the hole in a flat, hollow intensity profile fills in automatically due to diffraction after some distance. the easiest way to smooth such a profile is free space propagation. This is illustrated in Fig. 3 which shows a plane-wave with a circular cross-section of 20 cm diameter and a hole of 10 cm diameter propagating over a distance of 45 m. Each x-z plane in this pseudo-3D plot shows a radial intensity distribution (from -r to +r) for a different axial position y. After an irregular initial behavior with sharp axial spikes caused by edge diffraction, the emergence of a smooth, axially peaked profile is clearly visible. Some diverging side lobes which carry away energy from the central feature can also be observed. While a smooth profile can indeed be obtained in this way, especially if the side-lobes are now cut off with an appropriate aperture, the conversion efficiency of this process is obviously limited.

We have calculated the distances of propagation necessary to diffract a certain fraction of the initial beam intensity into the central lobe, for a range of initial beam profiles. The results are shown in Table I. Each hole diameter corresponds to the size of the

output coupler in a telescopic unstable resonator with a cavity feedback ε^2 of 5, 10, 15, 20 and 25% respectively. Note that ε is the ratio of the diameters of the two concentric circles bounding the beam profile.

The main conclusion from this table is the following: while the fill-in distances are not unreasonable - space for a 50 m long beam path can certainly be found in an experimental hall containing a plasma machine - the diffraction losses encountered are quite severe.

IV. DIRECT FOCUSING

Whether it is more important to avoid losses or to work with smooth intensity profiles depends on experimental parameters such as the laser power availabe, the access to the plasma machine and the construction of the beam dump. It has been pointed out earlier that the beam profile in the focal spot is satisfactory even in the case of focusing a ring-structured profile. The problem is that the beam emerges from the focal spot with a "memory" of its original shape.

In the following discussion we assume that an annular beam profile bounded by concentric circles of diameters d and $\varepsilon d (\varepsilon < 1)$ is focused by means of a lens of focal length f. We compare the beam profiles in the focal plane and in a plane at a distance f beyond the focal spot.

As beam qualifiers in the focal spot we use the half-width r_0 of the central lobe (radius of the first local intensity minimum), the

intensity ratio I_1/I_o of the peak of the first side lobe and the main lobe and the fraction E_o/E_{tot} of the total energy funneled into the central lobe. These parameters are shown in Fig. 4 as function of ε.

Based on the Fraunhofer diffraction theory,[6] this case can be treated analytically and thus provides a means of verifying the accuracy of the code. With the dimensionless variable $\rho = \pi dr/(\lambda f)$, the radial intensity distribution in the focal plane is obtained from

$$I(\rho) = 4/(1-\varepsilon^2)^2 \cdot \left[J_1(\rho)/\rho - \varepsilon^2 J_1(\varepsilon\rho)/\varepsilon\rho \right]^2 \cdot I_{in} \qquad (1)$$

where J is the Bessel function and I_{in} the intensity inside the original annulus. The fraction of the total energy contained in a disk of radius ρ_a is

$$E_a/E_{tot} = 1/2 \int^{\rho_a} (1-\varepsilon^2) I(\rho)/I_o \cdot \rho \, d\rho \qquad (2)$$

With increasing diameter of the hole in the annular intensity distribution, we observe in Fig. 4 the following effects: (i) the diameter of the central lobe decreases slightly, resulting in a somewhat improved resolution, (ii) the ratio of energy contained in the second and first maxima grows so that the contrast is reduced and (iii) more and more energy is diffracted outside the central lobe and is thus lost for the scattering process. For $\varepsilon > 0.3$ the focused energy decreases almost linearly with ε.

While the improved resolution, on the scale observed, is not significant in the context of Thomson scattering, the decreasing

contrast and mainly the loss of focused energy are rather severe. However, up to an ε-value of ~0.2 the curves are fairly flat. This means that the output of an unstble resonator with small feedback (~5%) can still be focused almost as well as a flat circular intensity profile. Recent experimental investigations[7] of a high power D_2O laser with an unstable resonator showed that the optimum feedback is indeed around 5%. From the point of view of the beam quality in the focal plane direct focusing is thus feasible.

To qualify the irregular beam profile emerging from the focal point is more difficult. We calculated the diameters of cross-sections containing 10, 20, 80 and 90% of the total intensity and define as beam qualifiers the ratios of these radii to the radius of a cross-section containing 50% of the total intensity.

In table II we list these qualifiers for a plane at a distance f beyond the focal point of a lens of focal length f. For comparison the same qualifiers are also shown for a thin annulus, as well as for a flat and a gaussian distribution. To dump a beam efficiently, a steeply decreasing profile, such as for example a gaussian, is desirable. In this case, the beam qualifiers span a large range. Their values are closer together for a profile with uniform intensity and are all equal for the worst possible case of an off-axial energy distribution. These observations serve as a guide on how to interpret table II from which we can draw the two following main conclusions: (i) it is easier to dump beams with small central holes and (ii) lenses of long focal length produce profiles with a flatter central part but steeper edges.

V. A PRACTICAL CASE

In our laboratory the design of an experiment to investigate the feasibility of measuring the ion temperature in the TCA tokamak is currently nearing completion. In this experiment the output radiation of an optically-pumped D_2O laser with an unstable resonator is focused into the torus by means of a 90 ° off-axis elliptical mirror. While this mirror was designed using 3D geometrical optics laws, we neglect in the following calculations the non-cylindrically symmetric aberration effects due to this mirror. The output of the FIR oscillator is sent through an intermediate focus with a telescopic mirror arrangement, as shown in Fig. 5. This has the following advantages: (i) the TPX window used to couple the FIR beam out of the tank containing the resonator can be much smaller and hence also thinner, reducing losses. (ii) fill-in propagation distances are reduced and (iii) apertures can be placed at the intermediate focal spot to improve the beam quality (spatial filtering).

Referring to Fig. 5, the beam transport starts with a ring-shaped intensity profile in plane P1 of outer diameter 20 cm and a 5 cm diameter hole. This fixes the diameters of mirrors M1 and M2. However, to avoid unnecessary diffraction losses we have chosen mirror M2 somewhat bigger: 25 cm diameter. We fix the radius of curvature of mirror M2 to 1 m. If M1, M2 formed a truly telescopic system, mirror M1, with a radius of curvature of 25 cm, would have to be placed at a distance of 37.5 cm from mirror M2. On the other hand, to obtain a focal spot in the center of mirror M2 the radius of curvature of mirror M1 should be 37.5 cm. Due to diffraction, however, the diameter of the beam inci-

dent on mirror M1 is larger than predicted by geometrical optics, resulting in additional losses. Increasing the distance M1-M2 reduces these losses but enhances the coupling losses through the hole in mirror M2. Careful optimization showed a mirror separation of 40 cm to be optimal. The radius of curvature of mirror M1 is obtained from geometrical optics considerations[8] according to equation

$$R_1 = 2d \frac{R_2 - 2d}{4d - R_2} \qquad (3)$$

where $R_{1,2}$ are the radii of curvature of the 2 mirrors and d the mirror separation. The size of the hole in mirror M2 has a two-fold influence on the transport efficiency in counteracting ways. A smaller hole results in a smaller aperture for the focused beam but in an increased reflecting mirror surface. We found numerically a hole diameter of 3.5 cm to be optimal.

In Fig. 5 we show the calculated intensity distribution incident on the planes P2, P1, P2 (intermediate focus), P3, P4 and P5, listed here in the order in which they are encountered following the beam trajectory. The focal length of mirror M3, which is shown as a lens in the drawing (Fig. 5), but is actually an elliptical mirror deflecting the beam by 90°, is 50 cm. For a fixed distance P2-P4 of 250 cm one obtains for P2-P3 180.9 cm and for P3-P4 69.1 cm.

We will now compare this arrangement to one without a telescopic system. Using the same focusing mirror M3 and the same distance P1-P4, one obtains an intensity distribution in the focal plane P4 which is not very different.

This is illustrated in table III where the beam qualifiers defined earlier are given for the two arrangements. The intensity contained in the central lobe in the focal plane P4 is 71.6% of the initial intensity for the telescopic system and 73.2% for the one-mirror arrangement. A significant difference is observed in plane P5 beyond the main focal spot (compare Figs. 6a and 6b). The requirements for a beam dump placed at this position are certainly relaxed considerably with the telescopic arrangement.

The transport efficiency with respect to the central lobe of the focal plane P4 is not reduced if an aperature for spatial filtering is placed in the hole of mirror M2, cutting off everything outside the main lobe. The improvement of the beam profile at the position of the beam dump (plane P5), however, is quite drastic (see Fig. 6c). In addition there are practically no side lobes in the focal plane P4.

In table III the four beam qualifiers defined earlier are given for the plane P5 beyond the focal point. From these numbers alone, without referring to figure 6, it follows that the distributions for the first two systems are relatively flat while the telescopic system with the aperture produces a distribution resembling a Gaussian (see also table II). It may not immediately be obvious why a Gaussian profile, incident on the beam dump, should be preferable to a flat one. While the intensity in a Gaussian profile decreases very rapdily with increasing distance from axis, the wings stretch to infinity. Indeed, if a truly rectangular distribution with sharp edges and zero intensity outside could be produced, this would be optimal for efficient dumping. However, in reality wings always exist. What is important is their rate of decrease which is optimum for Gaussian profiles.

VI. CONCLUSIONS

We have compared two beam transport codes and established the range of propagation distances over which they can be applied. The integral code was then used to investigate problems connected with the focusing of a beam with a ring-structured intensity profile. Tables were presented which allow one to estimate the distance of propagation necessary to fill in the hollow beam profile and to obtain information on the beam quality in and beyond the focal plane of a focusing element.

Finally, the beam transport system used to interface a D_2O laser with the TCA tokamak for an ion temperature measurement by Thomson scattering was investigated. It was found that a telescopic mirror system inside the FIR laser tank which creates an intermediate focus offers some important advantages. While the beam transport efficiency is not significantly degraded by its presence, the beam quality in the main focal plane and especially at the position of the beam dump is greatly improved.

This work was supported by the Swiss National Science Foundation and Euratom. We wish to thank P.D. Morgan for discussions and comments on this paper.

REFERENCES

1. A.E. Siegman, Applied Optics 13, 353-367 (1974).

2. M.R. Siegrist, M.R. Green, P.D. Morgan, R.L. Watterson, Applied Optics 19, 3824-3829 (1980).

3. W.H. Southwell, J. Opt. Soc. Am. 71, 7-14 (1981).

4. M.M. Johnson, Appl. Optics 13, 2326-2328 (1974).

5. P.D. Morgan, M.R. Green, M.R. Siegrist, R.L. Watterson, Comments Plasma Phys. Cont. Fusion 5, 141-157 (1979).

6. M. Born, E. Wolf, Principles of Optics, 4th ed., Pergamon Press, Oxford 1970. p. 416.

7. R. Behn, I. Kjelberg, P.D. Morgan, T. Okada, M.R. Siegrist, A High Power D_2O Laser Optimized for Microsecond Pulse Duration, Laboratory Report LRP 213/82 CRPP-EPFL, Lausanne 1982.

8. L.W. Casperson, Appl. Optics 20, 2243-2249 (1981).

FIGURE CAPTIONS

Fig. 1: Beam profiles of a flat annular intensity distribution (diameter 20 cm, hole diameter 10 cm) for propagation distances z of 2, 5, 10, 20, 50 m. Left hand side: integral method; right hand side: differential method.

Fig. 2: Focusing of a flat annular intensity distribution with a lens of f = 50 cm. Curve (1): initial profile, (2): profile in focal plane, (3): profile at distance f beyond focus.

Fig. 3: Free space propagation of a flat annular intensity distribution. Radial intensity profiles are shown for axial distances up to 45 m.

Fig. 4: Three beam qualifiers for the intensity distribution in the focal plane of a lens as a function of the size of the hole of an initially flat, annular profile. a) half width of central lobe, b) intensity ratio of the second and first maximum, c) fraction of energy contained in central lobe.

Fig. 5: Schematic of beam transport system for Thomson scattering measurements with an unstable resonator D_2O laser. A telescopic system allows to use a small output window and spatial filtering. Calculated radial beam profiles are shown for several positions.

Fig. 6: Beam profiles at the position of the beam dump for three beam transport systems (compare with Fig. 5): (a) direct focusing with element M3, (b) system shown in Fig. 5, (c) as (b) with aperture at P2.

Table I

Fill-in distances for annular beams of 20 cm external diameter

feedback of unstable resonator (%)	diameter of hole in beam (cm)	distance of propagation (m)	fraction of intensity in central lobe (%)
25	10	19	20
		25	30
		40	40
		∞	48
20	8.9	19	20
		24	30
		33	40
		68	50
		∞	54
15	7.7	18	20
		22	30
		28	40
		38	50
		∞	60
10	6.3	19	20
		22	30
		24	40
		30	50
		40	60
		∞	67
5	4.5	18	20
		20	30
		25	40
		31	50
		41	60
		∞	75

Table II

Beam qualifiers in the plane at distance 2f from the lens. Initial profile: flat, annular, 20 cm outer diameter.

cavity feedback of unstable resonator (%)	diameter of hole in beam (cm)	focal length (cm)	$\frac{r(I=10\%)}{r(I=50\%)}$	$\frac{r(I=20\%)}{r(I=50\%)}$	$\frac{r(I=80\%)}{r(I=50\%)}$	$\frac{r(I=90\%)}{r(I=50\%)}$
25	10	25	.74	.81	1.15	1.21
		50	.74	.81	1.13	1.20
		100	.74	.86	1.17	1.27
		200	.75	.84	1.18	1.39
20	8.9	25	.70	.77	1.17	1.22
		50	.71	.78	1.14	1.22
		100	.72	.82	1.18	1.29
		200	.73	.84	1.19	1.41
15	7.7	25	.65	.74	1.18	1.24
		50	.66	.75	1.17	1.24
		100	.68	.77	1.17	1.30
		200	.70	.84	1.22	1.42
10	6.3	25	.59	.72	1.20	1.26
		50	.61	.71	1.19	1.27
		100	.62	.73	1.18	1.29
		200	.64	.81	1.26	1.43
5	4.5	25	.52	.68	1.23	1.30
		50	.54	.68	1.22	1.30
		100	.55	.68	1.20	1.31
		200	.57	.76	1.27	1.45
Thin annular profile *)			1.	1.	1.	1.
Flat profile			.45	.63	1.26	1.34
Gaussian profile			.40	.58	1.44	1.63

*) Annulus of radii a and εa, with $\varepsilon \to 1$.

Table III

Beam qualifiers in the planes P4 (focus) and P5 (beam dump) for the system shown in Fig. 5

	r_o (mm)	transfer efficiency (%)	intensity ratio of lobes (%)	r(I=10%) / r(I=50%)	r(I=20%) / r(I=50%)	r(I=80%) / r(I=50%)	r(I=90%) / r(I=50%)
	referring to focal plane P4			referring to plane of beam dump P5			
System with one focusing mirror	1.1	73.2	3.6	.56	.68	1.19	1.27
System with telescope	1.6	71.6	2.8	.48	.67	1.29	1.48
System with telescope and aperture	1.9*	71.6	0.0	.40	.57	1.48	1.73

* this value is inaccurate. Since there are practically no side lobes, the intensity minimum between the central lobe and the first side lobe is not well defined. In fact, the central lobe is almost indistinguishable from the one without aperture.

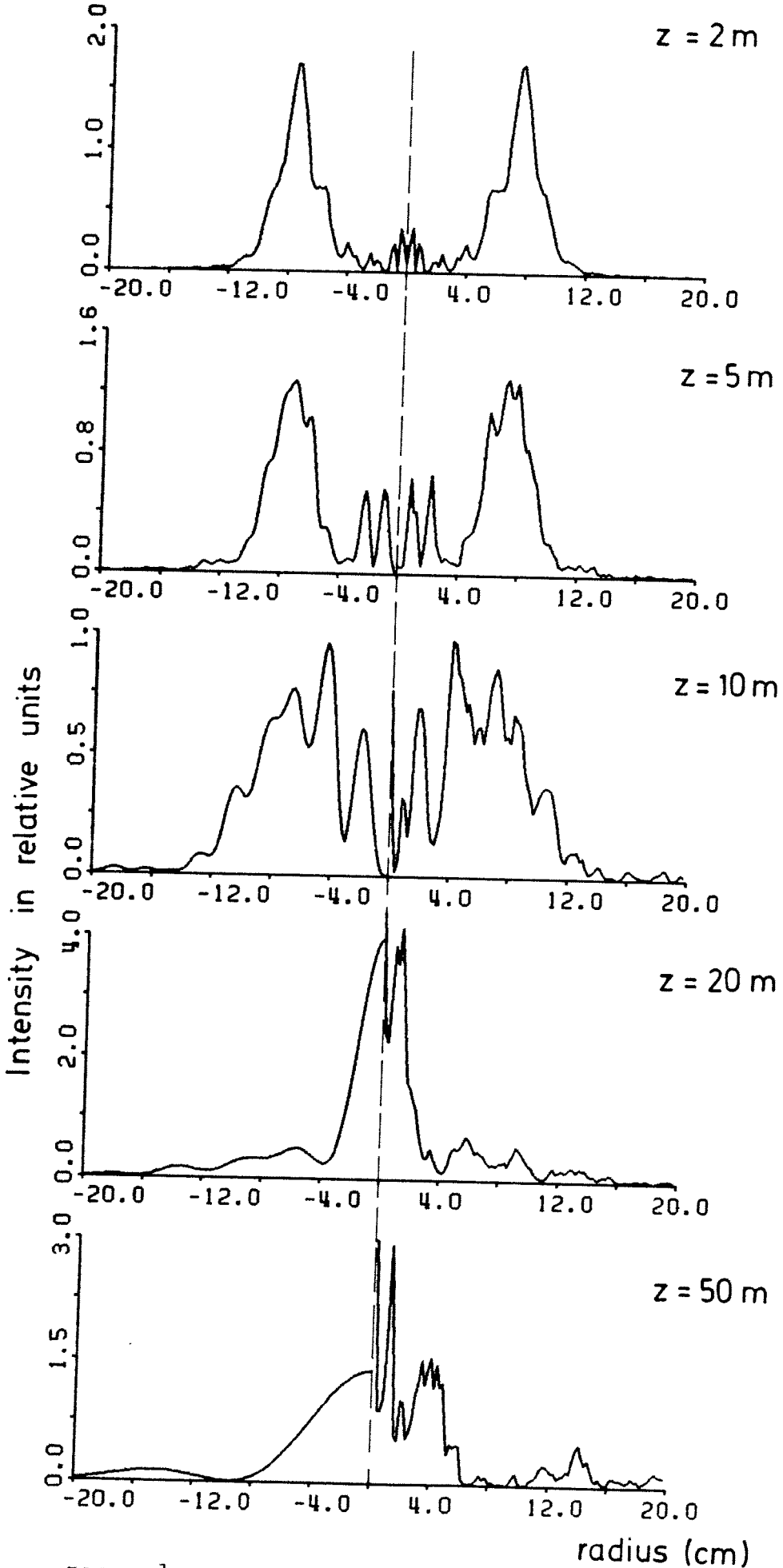
z = 2 m
z = 5 m
z = 10 m
z = 20 m
z = 50 m
Intensity in relative units
radius (cm)
-20.0
-12.0
-4.0
4.0
12.0
20.0

FIG. 1

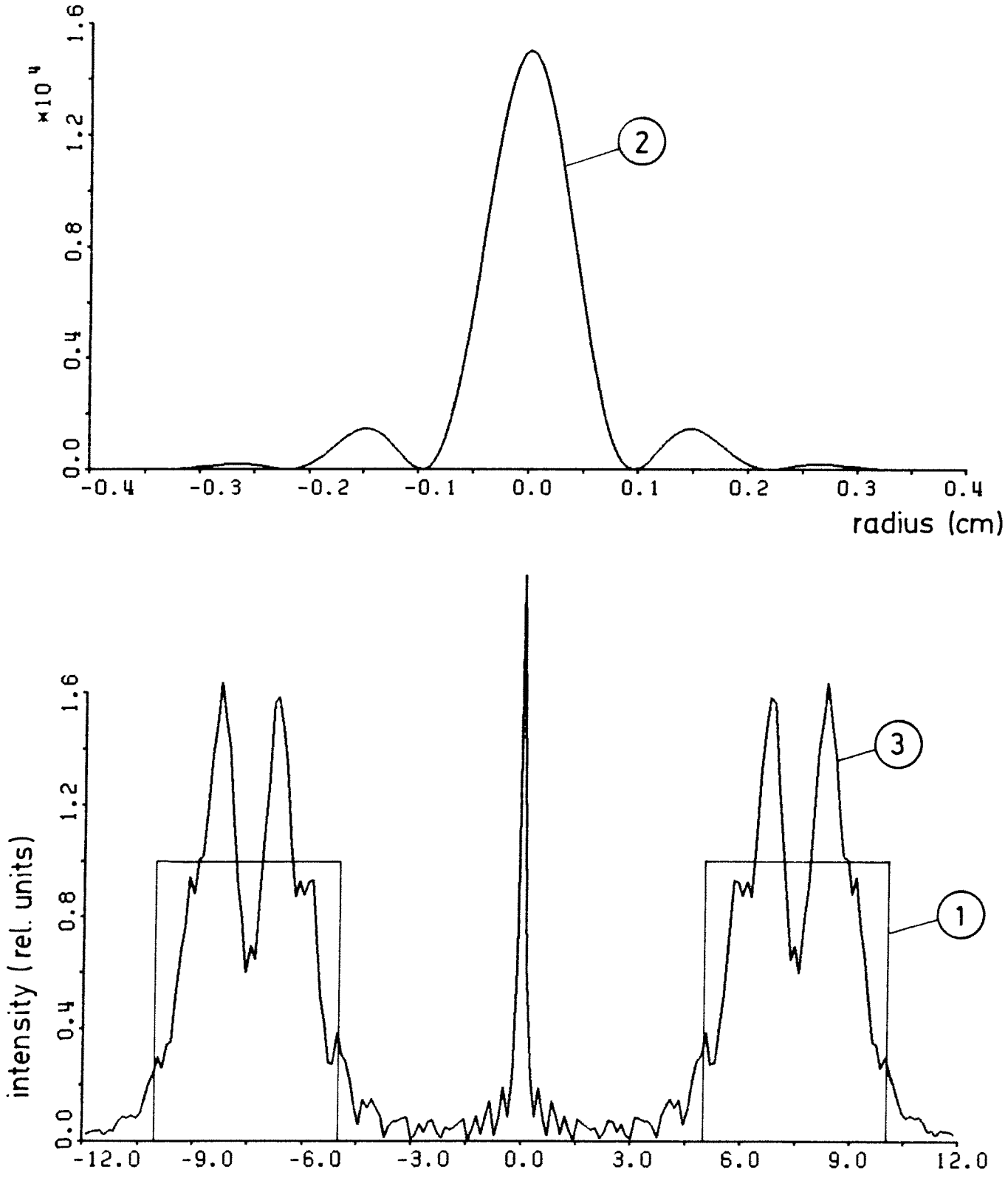
×10⁴
1.6
1.2
0.8
0.4
0.0
-0.4
-0.3
-0.2
-0.1
0.0
0.1
0.2
0.3
0.4
radius (cm)
2
intensity (rel. units)
1.6
1.2
0.8
0.4
0.0
-12.0
-9.0
-6.0
-3.0
0.0
3.0
6.0
9.0
12.0
3
1

FIG. 2

FIG. 3

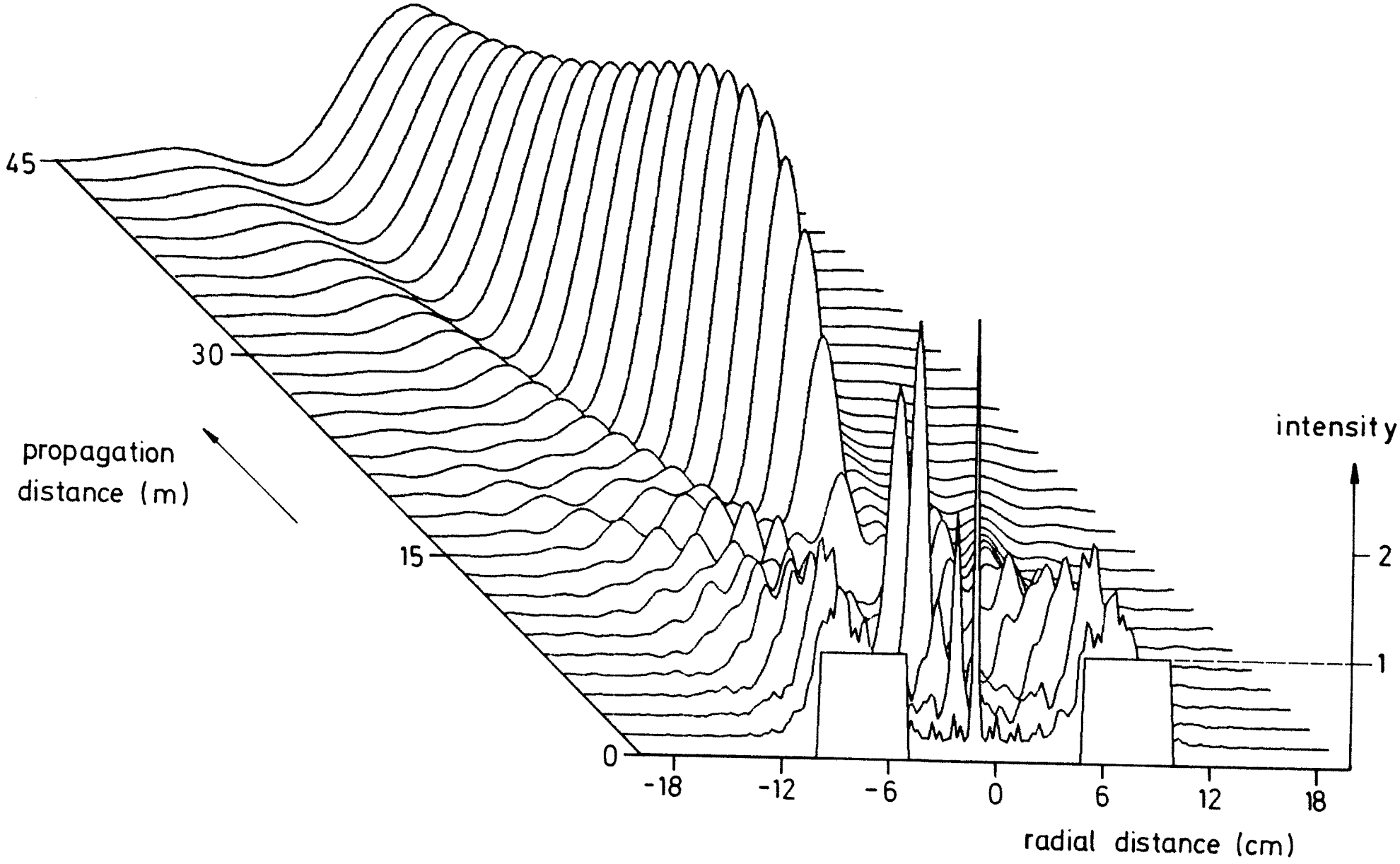
45
30
15
0
propagation
distance (m)
intensity
2
1
-18
-12
-6
0
6
12
18
radial distance (cm)

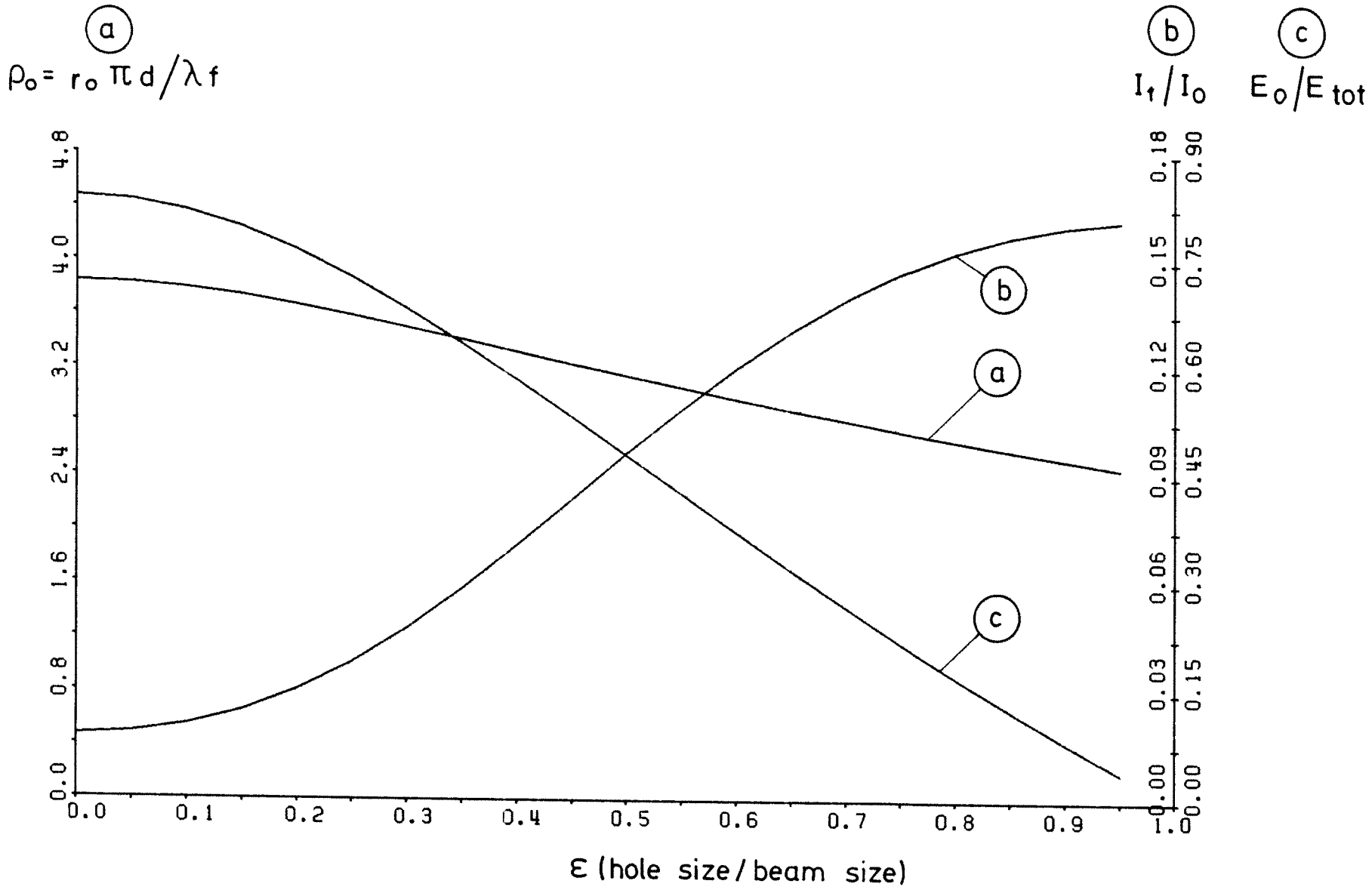
a
$\rho_o = r_o \pi d / \lambda f$
b
I_t / I_o
c
E_o / E_{tot}
4.8
4.0
3.2
2.4
1.6
0.8
0.0
0.18
0.15
0.12
0.09
0.06
0.03
0.00
0.90
0.75
0.60
0.45
0.30
0.15
0.00
0.0
0.1
0.2
0.3
0.4
0.5
0.6
0.7
0.8
0.9
1.0
b
a
c
ε (hole size / beam size)

FIG. 4

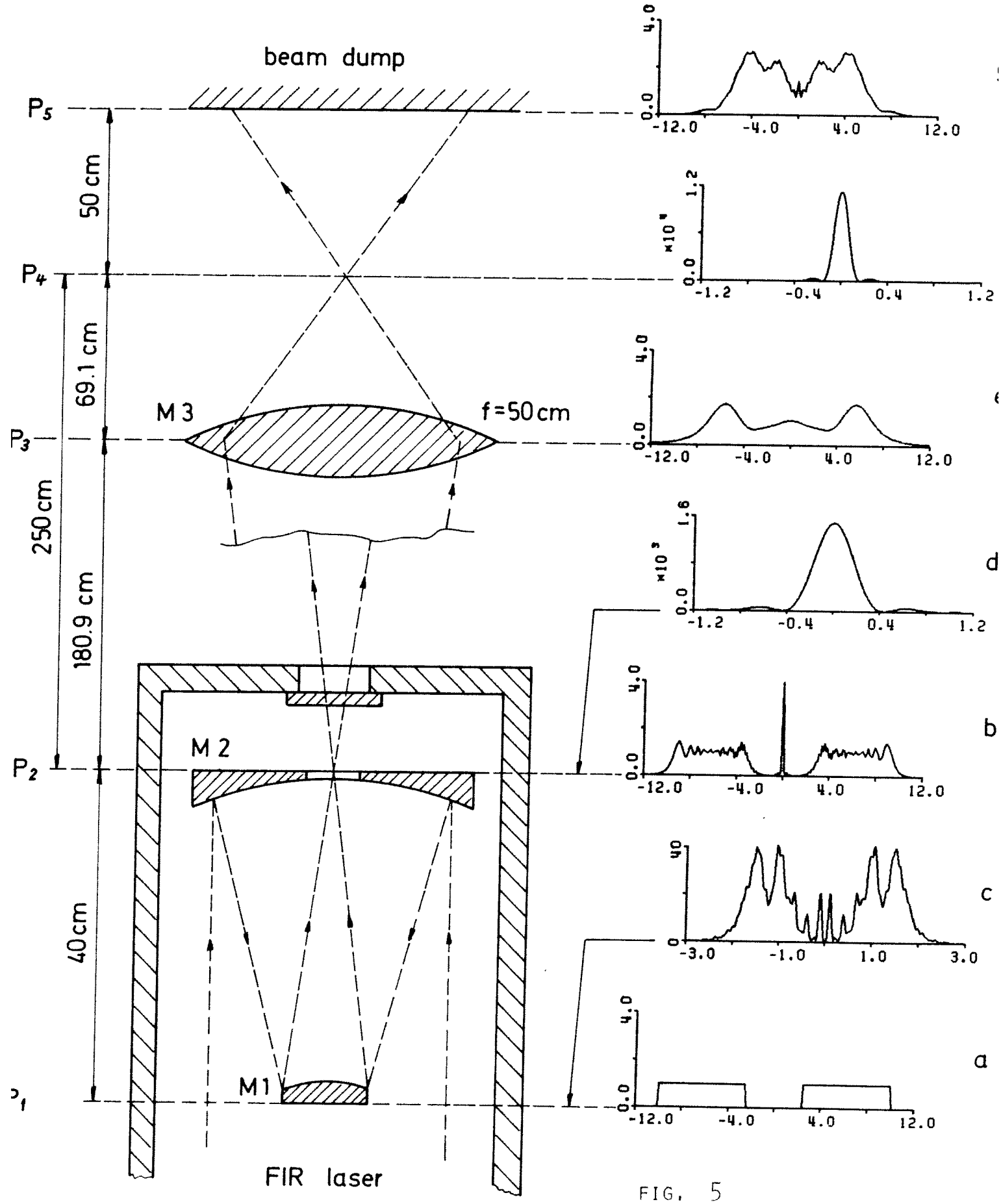
beam dump
P5
50 cm
P4
69.1 cm
M 3
f=50 cm
P3
250 cm
180.9 cm
M 2
P2
40 cm
M1
P1
FIR laser
4.0
0.0
-12.0
-4.0
4.0
12.0
1.2
×10³
-1.2
-0.4
0.4
1.2
d
1.6
b
-3.0
-1.0
1.0
3.0
c
a

FIG. 5

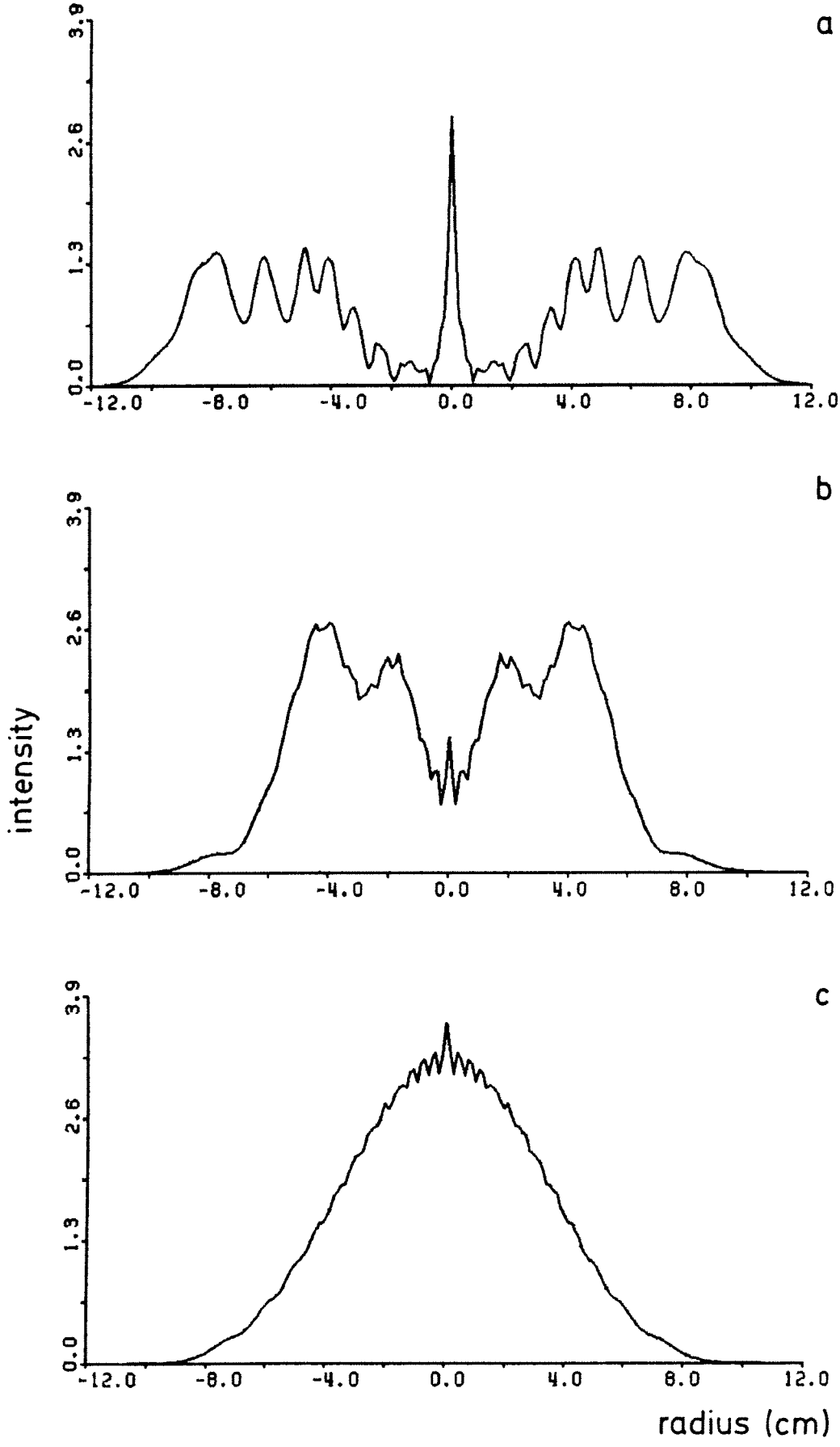

FIG. 6